Validation of Wind Turbine Wakes Modelled by the Meso-NH LES Solver Under Different Cases of Stability

E. Jézéquel, M. Cathelain, V. Masson, F. Blondel

▶ **To cite this version:**

E. Jézéquel, M. Cathelain, V. Masson, F. Blondel. Validation of Wind Turbine Wakes Modelled by the Meso-NH LES Solver Under Different Cases of Stability. Journal of Physics: Conference Series, 2021, 1934, pp.012003. 10.1088/1742-6596/1934/1/012003 . hal-03287414

HAL Id: hal-03287414
https://ifp.hal.science/hal-03287414

Submitted on 15 Jul 2021

HAL is a multi-disciplinary open access archive for the deposit and dissemination of scientific research documents, whether they are published or not. The documents may come from teaching and research institutions in France or abroad, or from public or private research centers.

L'archive ouverte pluridisciplinaire **HAL**, est destinée au dépôt et à la diffusion de documents scientifiques de niveau recherche, publiés ou non, émanant des établissements d'enseignement et de recherche français ou étrangers, des laboratoires publics ou privés.

Distributed under a Creative Commons Attribution 4.0 International License

Journal of Physics: Conference Series

PAPER • **OPEN ACCESS**

Validation of wind turbine wakes modelled by the Meso-NH LES solver under different cases of stability

To cite this article: E Jézéquel *et al* 2021 *J. Phys.: Conf. Ser.* **1934** 012003

View the article online for updates and enhancements.

IOP ebooks™

Bringing together innovative digital publishing with leading authors from the global scientific community.

Start exploring the collection–download the first chapter of every title for free.

This content was downloaded from IP address 109.0.19.194 on 09/07/2021 at 15:37

Validation of wind turbine wakes modelled by the Meso-NH LES solver under different cases of stability

E Jézéquel[1,2], M Cathelain[1], V Masson[2] and F Blondel[1]

[1] IFP Energies nouvelles, 1-4 Avenue de Bois Préau, Rueil-Malmaison, France
[2] Centre National de Recherches Météorologiques, 42 avenue Gaspard Coriolis, Toulouse, France

E-mail: erwan.jezequel@ifpen.fr

Abstract. In wind farms, the wakes of upstream turbines impact the downstream ones in terms of power production, loads, and fatigue. The wake properties depend on many parameters such as the stratification, Coriolis force, large-scale forcing and orography. To simulate this interdependence, the actuator line method (ALM) has been implemented in the atmospheric code Meso-NH, which is an LES research code developed by the French weather services. This implementation has already been validated for the blade force distribution on the NewMexico case (uniform inflow in a wind tunnel) and for the interaction with the atmosphere on the Horns Rev photo case. The work presented here aims at completing the validation in a realistic atmospheric boundary layer (ABL), with a focus on velocity deficit and wake meandering. It is based on the international SWiFT benchmark which compares the results of many numerical models with LiDAR measurements in the wake of a single turbine for three cases of atmospheric stability: neutral, unstable and stable. The good results show the capacity of Meso-NH/ALM to generate realistic wakes in a representative ABL.

1. Introduction

The wake behind a wind turbine is characterised by a decrease of wind velocity and an increased turbulence intensity (TI) compared to the inflow properties, leading respectively to a decreased generated power and increased unsteady loads for downstream turbines. The wake properties are impacted by the atmospheric boundary layer (ABL) in which the turbines are embedded. Shear and veer modify the wake shape [1], atmospheric stability influences the wake recovery [2] and the large eddies of the ABL induce wake meandering (oscillations of the instantaneous wake) [3]. An accurate description of the ABL is thus necessary to predict the wake properties.

The present work aims at demonstrating that Meso-NH with an actuator line method (ALM) [4] can be used to generate reference wake data for the calibration and validation of analytical models. Meso-NH is a meteorological solver that accounts for the aforementioned phenomena which can affect wind turbine's wakes. It can either be used in mesoscale or, as in this study, in large eddy simulation (LES) mode.

This work relies on a benchmark hereafter called SWiFT benchmark [5]. It is based on experiments where the wake of a stand-alone turbine over a flat terrain has been measured in three different atmospheric stability regimes: stable, neutral, unstable. The Meso-NH results are also compared to the LES codes of the benchmark: SOWFA (two simulations, hereafter denoted SOWFA and SOWFA-2), NaluWind, PALM, and EllipSys3D.


Content from this work may be used under the terms of the Creative Commons Attribution 3.0 licence. Any further distribution of this work must maintain attribution to the author(s) and the title of the work, journal citation and DOI.
Published under licence by IOP Publishing Ltd

2. The Meso-NH LES solver

Meso-NH (MESOscale Non Hydrostatic) is a finite volume, open-source research code for ABL simulations developed by the Centre National de Recherches Météorologiques and Laboratoire d'Aérologie. The first version of the model was introduced in [6], and recent updates in [7]. The unknowns are the velocities (U_x, U_y and U_z), the potential temperature θ and optionally the humidity which is not used here. The system of equations is a modified Navier-Stokes system with the following particularities:

- The equations use a constant density profile $\rho(z)$, and a buoyancy term is added to the momentum equation to take into account thermal effects.
- The equations are non-hydrostatic: the vertical pressure gradient term is not simplified with the gravity term.
- The Coriolis force is added to the momentum equation.
- The momentum equation is modified to take into account large-scale forcing through a geostrophic wind, which is imposed by the user.

In LES mode, an implicit low-pass filter is applied to the equations: the largest eddies of turbulence are directly resolved whereas the smallest must be modelled. In Meso-NH these eddies are modelled with a turbulence closure of order 1.5: an additional equation is introduced for the subgrid kinetic energy e_{sgs} and the other subgrid terms are modelled as functions of the resolved quantities, e_{sgs} and a mixing length L_m [8]. The mixing length is related to the grid size and stratification through the Deardorff formulation [9] for the neutral case or modified Deardorff formulation that works better in non-neutral conditions [10] for the stable and unstable cases. The spatial and temporal numerical schemes are respectively a fourth order centered and a fourth order Runge-Kunta. This leads to an accuracy of $4\Delta X$ [7], i.e. the smallest resolved turbulent structures is at best four times the mesh size.

An ALM representation of the wind turbine is employed, accounting for blade effect on the surrounding flow using rotating lines of source terms in the momentum equation, also called body forces [11]. The value of these body forces is computed with the blade element theory, relying on aerofoil data. This method has been implemented in Meso-NH, validated against the NewMexico experiments (a small turbine in a wind tunnel) and used to reproduce the Horns Rev photo case [4]. This early work was missing a quantitative validation of the coupled Meso-NH/ALM model in an actual ABL, which is the aim of the work presented hereby. It must be noted that in the literature, the forces are usually smeared with a gaussian kernel whereas in Meso-NH they are linearly smeared to the eight neighbouring cells.

The grid nesting technique allows to couple two or more computational domains of different sizes, temporal and spatial resolutions [12]. Hence, the resolution can be brought below the metre (necessary here in order to have 30 mesh-points per blade as recommended in [13]), while still taking into account the large-scale behaviour of the ABL.

3. Workflow

3.1. The SWiFT benchmark

The SWiFT measurements are performed on a 3-bladed horizontal axis wind turbine of diametre $D = 27$ m and hub height $z_{hub} = 32.1$ m. The location of the facility has two advantages: the orography can be neglected, and the atmospheric conditions are close to a canonical diurnal cycle [15]. The inflow conditions (reported in Table 1 for the three stability cases) are measured with a meteorological mast 65 m upstream the turbine and the velocity deficit in the wake is measured with a rear-facing, nacelle-mounted DTU SpinnerLidar [16], as schemed in Figure 1.

It is assumed that the beam elevation angle is zero and that the turbine is always aligned with the wind direction: consequently, the horizontal velocity is considered equal to the line-of-sight

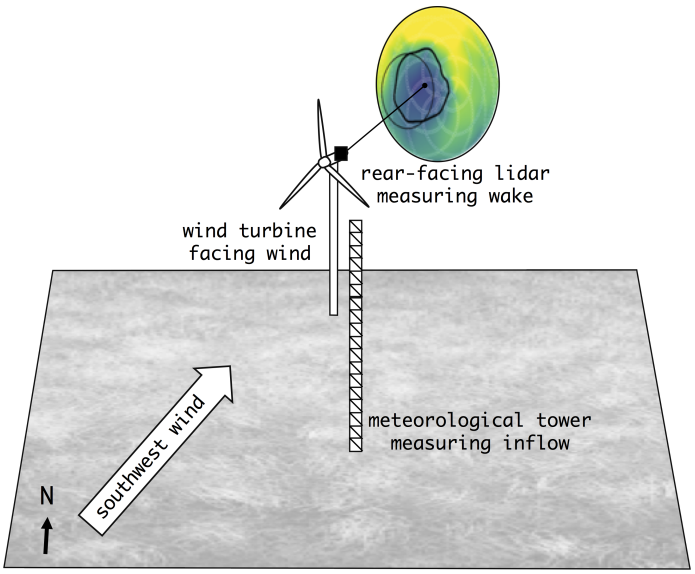

Figure 1: Schematic of the SWiFT facility used for this benchmark, from [14].

velocity [5]. The lidar sampling period was set to about 30–42 s for the neutral and stable cases, where the measurements focused on the spatial evolution of the mean wake. It was set to about 2 s in the unstable case in order to compute the estimate the dynamic behaviour such as wake meandering, but was restrained at one distance downstream ($x = 3D$) [17].

Table 1: Inflow conditions measured by the meteorological mast for the three cases. Performed at hub height (32 m) for $\overline{U}_{h,\infty}$ and TI and at 10 m for the others variables.

Variable	Notation	Unit	Neutral	Unstable	Stable
Horizontal inflow velocity	$\overline{U}_{h,\infty}$	[m/s]	8.7	6.7	4.8
Turbulence intensity	TI	[%]	10.7	12.6	3.4
Friction velocity	u_*	[m/s]	0.45	0.33	0.08
Stability parameter	$\zeta = z/L_{MO}$	[-]	0.004	–0.089	1.151
Kinematic vertical heat flux	$\overline{w'\theta'}$	[K.m/s]	–0.002	0.023	–0.005
Roughness length range	z_0	[mm]	5-50	5-50	5-50

3.2. Methodology

For each stability case we follow a three-step procedure:

- First it is necessary to properly reproduce the inflow conditions, focusing on the velocity and TKE profiles 65 m upstream the turbine. The *in-situ* measurements used a meteorological mast whereas the LES use time and lateral averaged profiles in a plane. In order to be consistent with the other data of the benchmark (both LES and measurements), we only use ensemble-averaged 10 minutes time-series of U_x, U_y and U_z, sampled at a frequency of 1 Hz. Consequently, the TKE profile does not take into account the subgrid quantities nor the contribution of eddies of frequency comprised outside the range from 1.67×10^{-3} Hz ($= 1/10$ min) to 1 Hz.

- Once the inflow is validated, the turbine model is integrated in the simulation. After 10 minutes of "spin-up" to let the wake and induction region establish, the wind turbine mean thrust coefficient and power are evaluated.
- Finally, the time-averaged velocity deficit in the wake is computed using the horizontal velocity in the inflow plane (thereafter noted $\overline{U}_{h,\infty}$) as a reference. The results are plotted as a function of the lateral (y) variable.

3.3. Numerical parameters

Table 2: Numerical parameters used in Meso-NH.

	Unit	Neutral				Unstable				Stable	
		D_1	D_2	D_3	D_4	D_1	D_2	D_3	D_4	D_1	D_2
z_0	[mm]	14				14				14	
$\overline{w'\theta'}$	[K.m/s]	–0.0020				0.0247				-0.0047	
ABL height	[m]	1000				1000				200	
Geostrophic wind	[m/s]	(u=11.35, v=-3.91)				(u=8.1, v=-1.2)				(u=7.6, v=-3.1)	
ΔZ	[m]	0.5				0.5				0.4	
$\Delta X = \Delta Y$	[m]	20	4	1	0.5	20	4	1	0.5	1.2	0.4
L_X	[m]	6400	2000	600	432	12000	3200	1000	450	540	360
L_Y	[m]	2400	800	240	162	6000	1600	500	225	300	150
Δt	[ms]	200	100	50	8	100	100	50	10	12	9
Cells number	[10^6]	7	18	27	52	46	82	128	104	35	105
Simulation time	[min]	80				20				10	
Ω	[rad/s]	4.56				3.89				2.79	
γ	[deg]	–0.75				–0.75				–0.75	

The numerical parameters used for the three simulations are presented in Table 2 for the different domains of the grid nesting. The size of the horizontal mesh depends on the domain D_i but in Meso-NH, the vertical mesh is the same for every domain. This is a major limitation which leads to flat cells near the ground, and to a needlessly large number of vertical mesh points in the large-scale domain D_1. In the region of the turbine and the wake, ΔZ is set in order to have isotropic cells in the most refined domain. The bottom boundary is determined by the subgrid momentum $\overline{w'u'}$ and heat fluxes $\overline{w'\theta'}$. The latter is prescribed and governs the evolution of θ in the middle of the first grid mesh, along with other resolved processes such as advection. The momentum flux influences the evolution of the wind at the same height. This subgrid momentum flux at the surface is computed according to the Monin-Obukhov laws, depending on the roughness length, wind at middle of first grid mesh and heat flux.

The flowfield is initialised with a constant-velocity profile equal to the geostrophic wind. A constant-temperature profile is set up to an arbitrary defined ABL height, capped by an inversion region (5K/50m). The geostrophic wind, ABL height, roughness surface and kinematic vertical heat flux are chosen in order to be as close as possible to the inflow measurements in terms of velocity, wind direction, TKE and stability parameter.

In the first domain D_1, the boundary conditions are cyclic in order to let the turbulence establish. The domain dimensions L_X and L_Y are chosen in order to be larger than the largest eddies of the flow, typically a couple of times the ABL height. The eddies are larger as the stability parameter ζ decreases: consequently a larger domain and four nested grids are needed

for the neutral and unstable simulations, whereas a small domain and two nested domains are enough for the stable one. The first step of the simulation is the initialisation of the ABL: the domain D_1 runs alone until the velocity spectra and the temperature and velocity profiles reach a steady state. Thirty hours are needed for the neutral case while a couple of hours are enough for the stable and unstable cases.

Then the nested domains (D_2, D_3 and D_4) are created, where the boundary conditions are interpolated from D_{i-1}. The domain size is constrained by the size of a turbulence build-up region: in each nested domain D_i, the eddies near the inlet are still at the size of the mesh of D_{i-1}. A spectral analysis has been carried out after each nesting to avoid this region for the next nested domain D_{i+1} or the turbine. It is not shown here for the sake of brevity but this procedure results into satisfying spectra upstream the turbine. Time step in every domain is driven by the CFL condition, except for the finest domain, where it is equal to the time needed for the tip of the blades to cross one cell. Without grid nesting, a mesh of $O(10^9)$ and a time step needlessly low for most of the domain would be needed for the neutral and convective cases.

Table 2 also shows the total time over which the ensemble averaging is performed (with all domains and ALM activated). It excludes a "spin-up" time arbitrarily set to 10 minutes to let the flow establish. In the measurements, the ensemble averaging is done over six segments of 10 minutes for the neutral and stable cases and five segments for the unstable case. In Meso-NH, an ensemble-average over eight segments (80 minutes) was targeted but due to unsteadiness it had to be reduced for the stable and unstable cases.

The rotational velocity of the wind turbine Ω and pitch of the blade γ are set constant to a value interpolated in the controller table of the turbine with $\overline{U}_{h,\infty}$ defined in Table 1. It must be acknowledged that some other models use a more realistic controller which adapts Ω and γ during the simulation. The Glauert correction for tip loss is used [4]. The velocity at every blade node is interpolated with the eight neighbouring cells. A simple implementation of the nacelle and the tower is used, even though it is not clear if these elements were included in the other LES of the benchmark.

4. Results

4.1. Inflow

The inflow horizontal velocity $\overline{U}_{h,\infty}$ and TKE e_∞ measured in the benchmark cannot be directly prescribed in Meso-NH. Instead, the user must find appropriate values for the geostrophic wind, the initial conditions and the ground forcing ($\overline{w'\theta'}$, z_0, u_*) that lead to the desired inflow profiles.

The stable case is actually a strongly stable case, with $\zeta = 1.151$ at 10 m. The ABL under such stable conditions is complex to simulate because the nature of turbulence is changed, leading to the failure of usual turbulence models. A value of $\zeta = 0.4$ has been reached in Meso-NH. A better match is achievable, but would have needed a finer mesh in the domain D_1 (estimated around 0.8 m). Conversely, the unstable case can be considered as a weakly convective case ($|\zeta| \approx |Ri| < 0.3$ [18]) and thus the physics should not be too different from the neutral case.

The inflow horizontal velocity profiles computed by Meso-NH, compared to the ones of the benchmark are plotted in Figures 2a, 2b, and 2c (respectively for the neutral, unstable and stable benchmarks). For the neutral and unstable cases, they are similar to the measured profiles and to the inflow profiles of the other simulations. For the stable case, the shear in Meso-NH is lower than the measurements and SOWFA. This can be explained by the fact that the stability parameter is not reached in our simulation.

The TKE profile for the neutral case (Figure 3a) is very satisfying, with a better shape and amplitude than the other codes compared to the measurements. For the unstable (Figure 3b), and stable (Figure 3c) cases, the Meso-NH TKE profiles are similar to the other LES and slightly lower than the measurements.

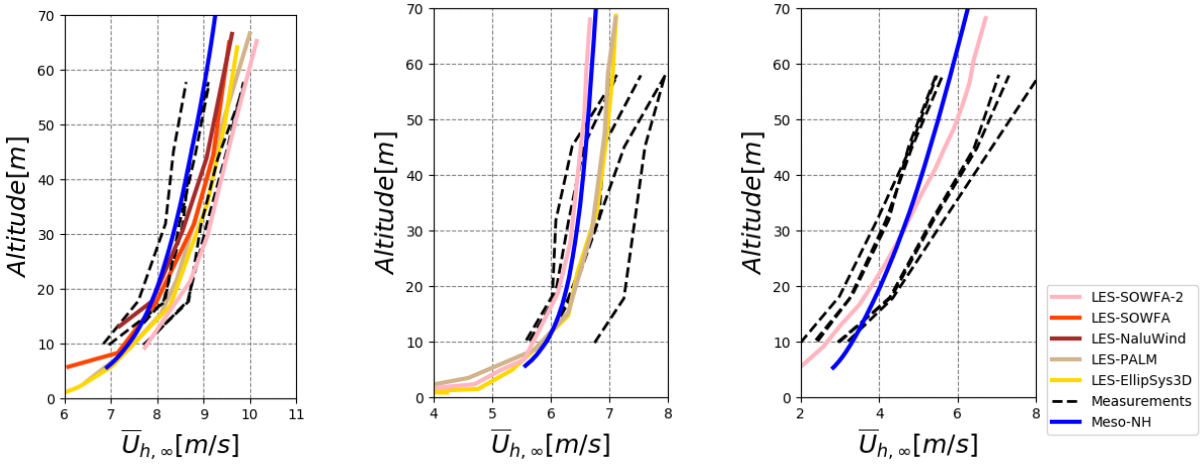

(a) Neutral case (b) Unstable case (c) Stable case

Figure 2: Horizontal velocity at the inflow.

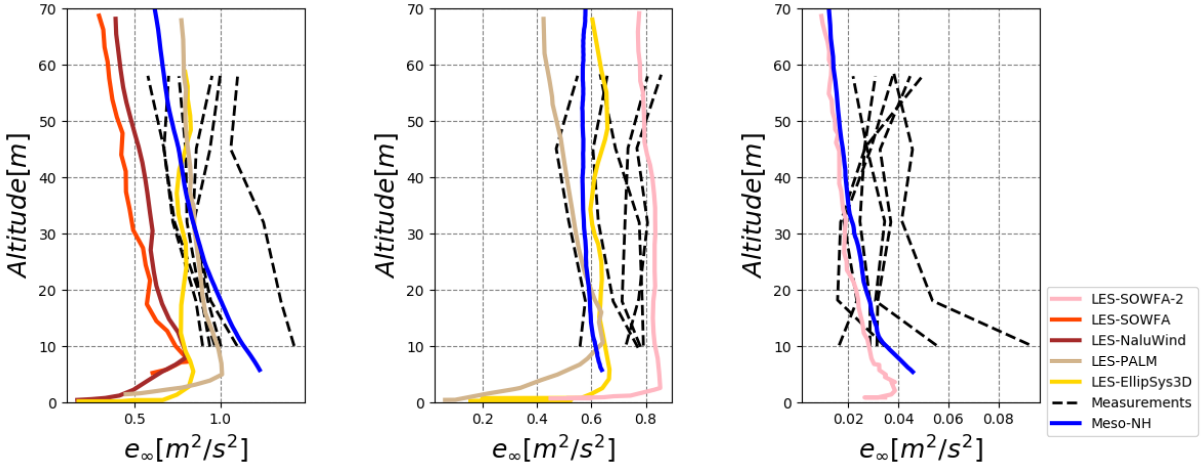

(a) Neutral case (b) Unstable case (c) Stable case

Figure 3: Horizontal TKE at the inflow.

4.2. Turbine response

The mean turbine response for the three cases is given in Figures 4a and 4b. We analyse the generator's power P_{gen} and the thrust coefficient defined by:

$$C_T = \frac{T}{\frac{1}{2}\rho A U_{h,\infty}^2} \tag{1}$$

where T is the total thrust of the turbine, ρ is the density of air, and A the swept rotor area. The wake velocity deficit is mainly due to the thrust of the turbine, so it is the most important variable for us. Unfortunately, it could not be measured on the full-scale turbine, so Meso-NH's results will only be compared to the other LES codes.

Regarding the neutral case, Meso-NH gives a thrust value similar to the other LES codes. Less numerical models have taken part to the two other benchmarks, so it is difficult to compare

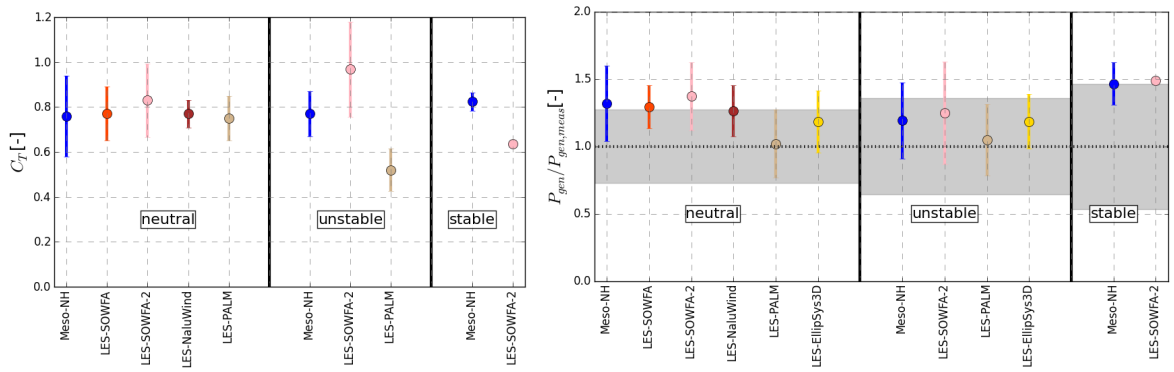

(a) Thrust coefficient. No *in-situ* measurements were available.

(b) Generator power, normalised by the measured generator power. The grey region underlines the standard deviation of the measurements.

Figure 4: 10-minute averaged turbine response of every code for the three benchmarks, with error bars to highlight the standard deviation.

the results in absence of thrust measurements. The power, in Meso-NH like in the other LES, is always overestimated compared to the measurements. It comes from a torque overestimation that has not been explicitly explained in the original publication [5] but it is supposed to be of secondary importance for the wake velocity deficit study since the thrust is the main driver. It remains a subject of concern for our validation.

4.3. Velocity deficit

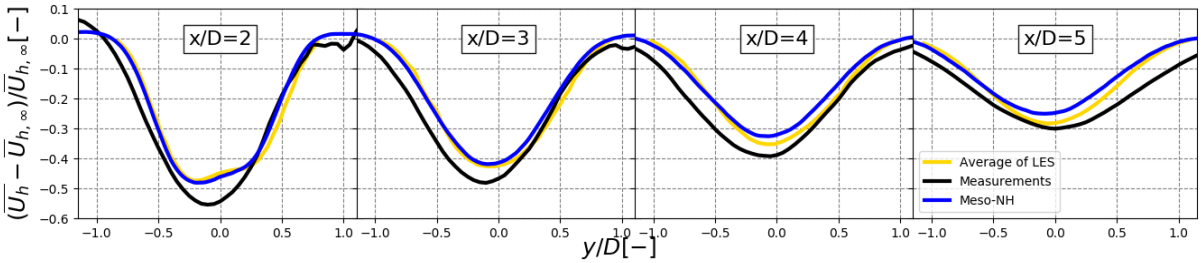

Figure 5: Velocity deficit profiles in the horizontal plane at hub height for the neutral case. The other LES results of this case have been collapsed into one single curve (yellow).

For the neutral case, the time-averaged velocity deficit profiles at hub height in the wake of the turbine are plotted in Figure 5 at four planes (2, 3, 4 and 5 diametres downstream the turbine). For the sake of clarity, the ensemble average of the five LES of the benchmark is plotted (yellow curve), along with the measurements and Meso-NH results. At $x = 2D$ the maximum deficit and wake width is very similar between Meso-NH and the other LES, which is consistent with the fact that the thrust coefficients are in the same range. The wake then dissipates slightly faster in Meso-NH than in the other codes, at a rate similar to the measurements: this can be explained by the inflow TKE in Meso-NH being close to the measurements and higher than in the other LES (Figure 3a). Overall, the behaviour of the wake is thus consistent with the incoming flow field and turbine response.

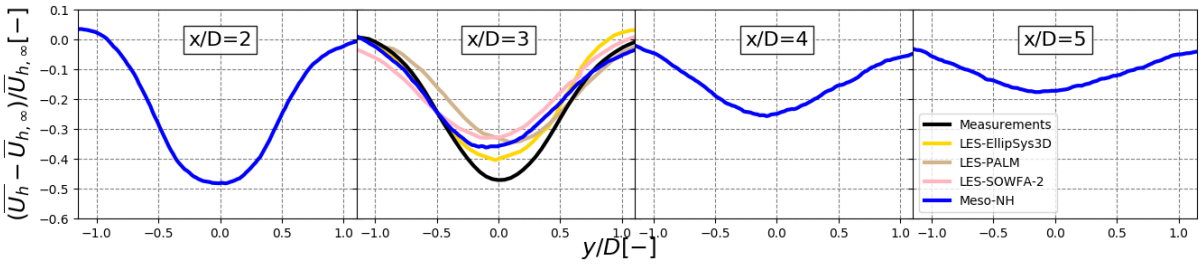

Figure 6: Velocity deficit profiles in the horizontal plane at hub height for the unstable case.

The unstable case is focusing on the wake deficit three diametres downstream the turbine (Figure 6). At first sight, it appears that the wake in Meso-NH and EllipSys3D are better than those of SOWFA-2 and PALM. However, when the meandering motion is removed, all the simulations give results very similar to the measurements (not shown here for brevity). The discrepancies observed here can thus be interpreted as the consequence of differences in wake meandering (see next section) and not in the wake itself.

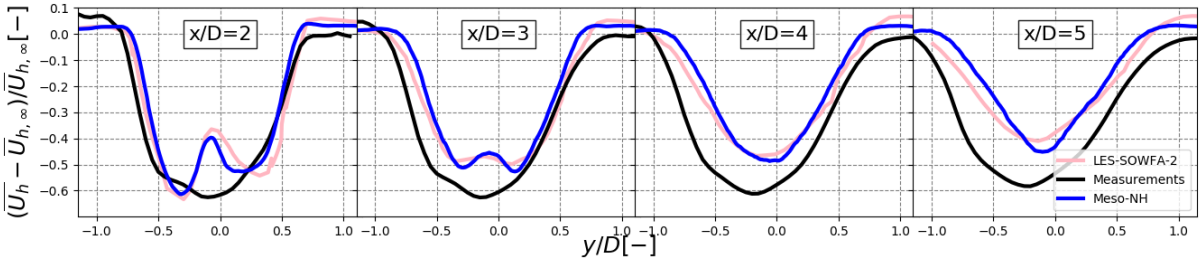

Figure 7: Velocity deficit profiles in the horizontal plane at hub height for the stable case.

Despite strong differences in thrust coefficients, the velocity deficit in the stable case (Figure 7) is very similar between Meso-NH and SOWFA-2 excepted at $x = 5D$ where the Meso-NH's wake is narrower and has a slightly larger velocity deficit. For both LES, the wake dissipates faster than in the measurements, despite correct values of inflow TKE (Figure 3c). This highlights the difficulty of numerical codes and measurements to operate in a strongly stable atmosphere.

4.4. Wake meandering

In this work the horizontal wake meandering is quantified as:

$$\Gamma_y(x) = \frac{\sqrt{\overline{y_c'^2}}}{D} \tag{2}$$

where $\overline{y_c'^2}$ is the variance of the horizontal position of the wake centre. The vertical wake meandering $\Gamma_z(x)$ is similarly defined. To find the position of the wake centre at each time step, the methodology of the SWiFT benchmark [5] is followed in order to have the same post-processing and comparable results: a 2D Gaussian curve is fitted on the velocity deficit at each time step [19]. After removing spurious positions, a median filter is applied to the time series of the wake position.

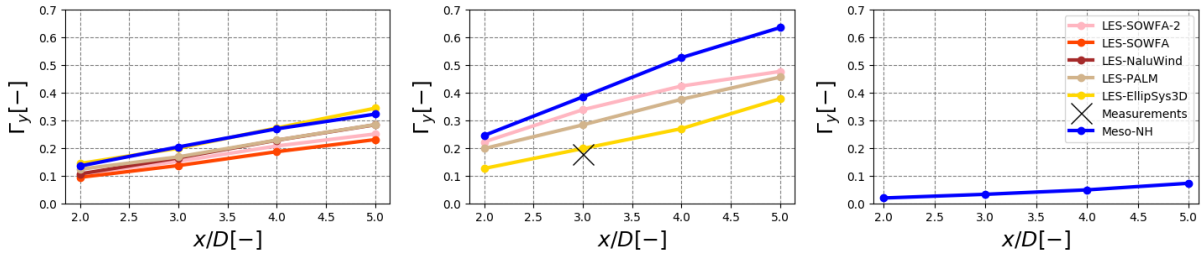

(a) Neutral case (b) Unstable case (c) Stable case

Figure 8: Horizontal wake meandering.

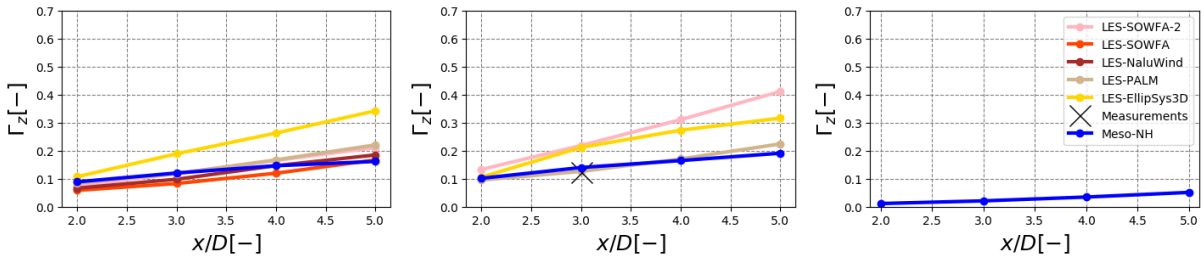

(a) Neutral case (b) Unstable case (c) Stable case

Figure 9: Vertical wake meandering.

The horizontal and vertical wake meandering are plotted for every case in Figures 8a to 9c as a function of x/D. Measurements are only available for the unstable case at $x = 3D$, where they are in good agreement with Meso-NH for the vertical direction (Figure 9b). Conversely, the amplitude of the horizontal meandering in Meso-NH is twice the value of the *in-situ* measurements. Even though the other codes also overestimate the horizontal meandering, Meso-NH is always among the codes predicting the strongest meandering in this direction.

For every case the horizontal wake meandering is stronger than the vertical one, a phenomenon attributed to the presence of the ground that prevents the formation of large eddies. Also, the wake meandering decreases as the stability increases. Despite having one single point of validation at $x = 3D$ the general behaviour of the wake meandering in Meso-NH is consistent with a previous LES study on the subject [2].

5. Conclusion

The newly implemented actuator line method in Meso-NH has been compared to the *in-situ* measurements and LES simulations of the SWiFT benchmark. For the three cases (near neutral, weakly unstable and strongly stable), the turbine's power and thrust, the near-wake ($x = 2D$ to $x = 5D$) velocity deficit, and meandering have been evaluated. All the Meso-NH simulations gave promising results even though the stable case was at the edge of the code's capacities.

The slight overestimation of the generated power in Meso-NH can be linked to similar observations of the code's tangential efforts on the blades [4]. It might be due to the smearing of the forces that is used, which is not the one recommended in the literature. For every case the thrust coefficient and velocity deficit in the wake are satisfying when compared to the other codes. Similarly to the SOWFA simulation, the wake in Meso-NH is dissipating too quickly in the stable case compared to measurements. Finally the wake meandering in the horizontal direction in Meso-NH is among the highest values of other codes. Conversely, in the vertical direction it is among the lowest values and fits well the measurements for the unstable case at

$x/D = 3$.

As a conclusion, we can consider that the coupling Meso-NH/ALM is validated for wakes in stratified ABLs. It will now be possible to use it as a tool to quantify the effect of the ABL (e.g. stratification and surface roughness) on the wake, and in particular on the added turbulence.

Acknowledgments

The authors would like to thank P. Doubrawa for providing the data of the three SWiFT cases and the LES modellers of the benchmark (S. Krüger, D.C Maniaci, M. Debnath and S.J Andersen) for allowing the use of their data. They would also like to thank E. Quon for helping to perform the wake tracking with his SAMWICH toolbox. This work was granted access to the HPC resources of TGCC under the allocation 2020- A0092A12008 made by GENCI.

References

[1] Englberger A, Dörnbrack A and Lundquist J K Does the rotational direction of a wind turbine impact the wake in a stably stratified atmospheric boundary layer? 2020 *Wind Energy Science* **5** 1359–1374
[2] Abkar M and Porté-Agel F Influence of atmospheric stability on wind-turbine wakes: A large-eddy simulation study 2015 *Physics of Fluids* **27** 035104
[3] Larsen G C, Madsen H A, Thomsen K and Larsen T J Wake meandering: a pragmatic approach 2008 *Wind Energy* **11** 377–395
[4] Joulin P A, Mayol M L, Masson V, Blondel F, Rodier Q, Cathelain M and Lac C The actuator line method in the meteorological LES model meso-NH to analyze the horns rev 1 wind farm photo case 2020 *Frontiers in Earth Science* **7**
[5] Doubrawa P, Quon E W, Martinez-Tossas L A, Shaler K, Debnath M, Hamilton N, Herges T G, Maniaci D, Kelley C L *et al.* Multimodel validation of single wakes in neutral and stratified atmospheric conditions 2020 *Wind Energy*
[6] Lafore J P, Stein J, Asencio N, Bougeault P, Ducrocq V, Duron J, Fischer C, Héreil P, Mascart P *et al.* The meso-NH atmospheric simulation system. part i: adiabatic formulation and control simulations 1998 *Annales Geophysicae* **16** 90–109
[7] Lac C, Chaboureau J P, Masson V, Pinty J P, Tulet P, Escobar J, Leriche M, Barthe C, Aouizerats B *et al.* Overview of the meso-NH model version 5.4 and its applications 2018 *Geoscientific Model Development* **11** 1929–1969
[8] Cuxart J, Bougeault P and Redelsperger J L A turbulence scheme allowing for mesoscale and large-eddy simulations 2000 *Quarterly Journal of the Royal Meteorological Society* **126** 1–30
[9] Deardorff J W Stratocumulus-capped mixed layers derived from a three-dimensional model 1980 *Boundary-Layer Meteorology* **18** 495–527
[10] Honnert R, Masson V, Lac C and Nagel T A theoretical analysis of mixing length for atmospheric models from micro to large scales 2021 *Frontiers in Earth Science*
[11] Sørensen J N and Shen W Z Numerical modeling of wind turbine wakes 2002 *Journal of Fluids Engineering* **124** 393–399
[12] Stein J, Richard E, Lafore J P, Pinty J P, Asencio N and Cosma S High-resolution non-hydrostatic simulations of flash-flood episodes with grid-nesting and ice-phase parameterization 2000 *Meteorology and Atmospheric Physics* **72** 203–221
[13] Jha P K, Churchfield M J, Moriarty P J and Schmitz S Guidelines for volume force distributions within actuator line modeling of wind turbines on large-eddy simulation-type grids 2014 *Journal of Solar Energy Engineering* **136** 031003
[14] `https://wakebench-swift.readthedocs.io/en/latest/measurements.html` accessed: 2021-04-07
[15] Kelley C L and Ennis B L 2016 SWiFT site atmospheric characterization Tech. rep.
[16] Mikkelsen T, Angelou N, Hansen K, Sjöholm M, Harris M, Slinger C, Hadley P, Scullion R, Ellis G and Vives G A spinner-integrated wind lidar for enhanced wind turbine control 2012 *Wind Energy* **16** 625–643
[17] Doubrawa P, Debnath M, Moriarty P J, Branlard E, Herges T G, Maniaci D C and Naughton B Benchmarks for model validation based on LiDAR wake measurements 2019 *Journal of Physics: Conference Series* **1256** 012024
[18] Stull R B (ed) 1988 *An Introduction to Boundary Layer Meteorology* (Springer Netherlands)
[19] Quon E W, Doubrawa P and Debnath M Comparison of rotor wake identification and characterization methods for the analysis of wake dynamics and evolution 2020 *Journal of Physics: Conference Series* **1452** 012070